DMD Fast Forward. Published on June 27, 2012 as doi:10.1124/dmd.112.045872

A Commentary: Theoretical Predictions of Flow Effects on Intestinal (F_I) and Systemic Availability (F_{sys}) in PBPK Intestine Models: The Traditional Model (TM), Segregated Flow Model (SFM) and Q_{Gut} Model

K. Sandy Pang and Edwin C.Y. Chow

Leslie Dan Faculty of Pharmacy, University of Toronto, Toronto, Ontario, Canada, M3S 3M2

Running Title: Intestinal flow models in PBPK modeling

Correspondence: Dr. K. Sandy Pang
Leslie Dan Faculty of Pharmacy, University of Toronto
144 College Street, Toronto
Ontario, Canada M5S 3M2
TEL: 416-978-6164
FAX: 416-978-8511
E-mail: ks.pang@utoronto.ca

Abstract: 242 words

Introduction: 745 words

Discussion: 891 words

References: 58

Figures: 5

Table: 0

DMD Fast Forward. Published on June 27, 2012 as DOI: 10.1124/dmd.112.045872
This article has not been copyedited and formatted. The final version may differ from this version.

Glossary

AUC	area under the curve
C_A	arterial concentration
$\overline{C}_{PV}$	flow-averaged portal venous concentration
CL_{d1}, CL_{d2}, CL_{d3} and CL_{d4}	influx and effect intrinsic clearances
$CL_{int,I}$	total, intestinal intrinsic clearance
$CL_{int,met1}$ and $CL_{int,met2}$	metabolic intrinsic clearances
$CL_{int,sec}$	intrinsic clearance for secretion
CL_{perm}	drug permeability clearance
E	extraction ratio
F_I, F_H, F_{sys}	intestinal, hepatic and systemic availability
f_B, f_I and f_H	unbound fraction in blood, intestine, and liver
f_Q	fractional flow rate to the enterocyte region
GIT	gastrointestinal tract
k_a and k_g	absorption and luminal degradation rate constant
P_{app}	apparent permeability
P_{eff}	effective permeability
PBPK	physiologically based pharmacokinetic
po and iv	oral and intravenous administration
Q_{gut}	effective flow
Q_{villi}	villous flow
SFM	segregated flow model
SSFM	segmental segregated flow model
STM	segmental traditional model
TM	traditional model
v_I and v_H	rate of intestinal and hepatic removal

DMD Fast Forward. Published on June 27, 2012 as DOI: 10.1124/dmd.112.045872
This article has not been copyedited and formatted. The final version may differ from this version.

Abstract

PBPK models for the intestine, comprising of different flow rates perfusing the enterocyte region, were revisited in the appraisal of flow affects on the intestinal availability (F_I) and in turn, the systemic availability (F_{sys}) and intestinal vs. liver contribution to the first-pass effect during oral drug absorption. The traditional model (TM), the segregated flow model (SFM) and the Q_{Gut} model, respectively, stipulate that 1.0x, ~0.1x to 0.3x and ≤ 0.484x of the total intestinal flow, respectively, reach the enterocyte region which houses metabolically-active and transporter-enriched enterocytes. The fractional flow rate to the enterocyte region, f_Q, when examined under varying experimental conditions, was found to range from 0.024 to 0.2 for the SFM and 0.065 to 0.43 for the Q_{Gut} model. Appraisal of these flow intestinal models, when used in combination with whole body-physiological-based pharmacokinetic (PBPK) models, showed the ranking was SFM < Q_{Gut} model < TM in the description of F_I, and the same ranking existed for the contribution of the intestine to first-pass removal. But the ranking for the predicted contribution of hepatic metabolism to first-pass removal was opposite: SFM > Q_{Gut} model > TM. The findings suggest that the f_Q value strongly influences the rate of intestinal metabolism, F_I and F_{sys}, and indirectly affects the rate of liver metabolism due to substrate sparing effect. Thus, the f_Q value in the intestinal flow model poses serious implications on the interpretation of data on the first-pass effect and oral absorption of drugs.

DMD Fast Forward. Published on June 27, 2012 as DOI: 10.1124/dmd.112.045872
This article has not been copyedited and formatted. The final version may differ from this version.

INTRODUCTION

Compartmental models are no longer adequate to address effects of permeability barriers (de Lannoy and Pang, 1986; de Lannoy and Pang, 1987), intestinal and liver transporters and enzymes (Suzuki and Sugiyama, 2000a; 2000b), and sequential metabolism within the intestine and liver (Pang and Gillette, 1979; Sun and Pang, 2010) during oral drug absorption (for reviews, see Pang, 2003; Pang et al., 2008; Fan et al., 2010; Pang and Durk, 2010; Chow and Pang, 2012). These aspects are especially pertinent when intestinal metabolic activity is substantial relative to that in the liver, and when different extents of induction/inhibition of intestinal and hepatic enzymes or transporters result upon treatment of the culprit compound, usually showing a higher induction/inhibition effect with oral administration (Fromm et al., 1996; Paine et al., 1996; Thummel et al., 1996; Eeckhoudt et al., 2002; Mouly et al., 2002; Fang and Zhang, 2010; Liu et al., 2010; Lledó-García et al., 2011; Zhu et al., 2011).

Over the past decade, there have been exciting advances made towards the development of physiologically-relevant PBPK intestinal models to inter-relate intestinal transporters, enzymes and blood flow in the appraisal of their influence on intestinal (F_I), liver (F_H), and oral systemic (F_{sys} or $F_{abs}F_IF_H$) availability. In this commentary, we revisited several physiologically-based intestinal models that are associated with differential flow patterns: the traditional model, TM, in which the entire intestinal flow perfuses the enterocyte region, the segregated flow model, SFM, in which a low enterocyte flow, Q_{en}, perfuses the enterocyte region (fractional flow, f_Q or Q_{en}/Q_{PV} is ≤ 0.3) (Cong et al., 2000), and the Q_{Gut} model, in which the effective flow Q_{Gut} that perfuses the enterocyte region is at best half the intestinal flow and close in value to the villous flow, Q_{villi} (Yang et al., 2006; Yang et al., 2007; Gertz et al., 2010). These three intestinal models are viewed as competent to describe the immediate removal of the formed metabolite by excretion or

sequential metabolism within the intestine and/or further processing by liver, for drugs and metabolites exhibiting varying permeability properties (Cong et al., 2000; Yang et al., 2006; 2007; Gertz et al., 2010; Sun and Pang, 2010). The models are more prepared to supply mechanistic insight on the pharmacokinetics of drugs and their metabolites and allow inclusion of transporters into different organ components (apical or basolateral membranes) to discriminate between the permeability properties of the drug and its formed metabolite in permitting or delimiting influx and efflux in drug and metabolite processing (Pang et al., 2008; Darwich et al., 2010; Galetin et al., 2010; Gertz et al., 2010; Rowland Yeo et al., 2010; Chow and Pang, 2012). By virtue of inclusion of transport and eliminatory events, these physiologically-based models are able to describe more accurately the net appearance of the formed metabolite into the systemic circulation, since metabolite levels can be drastically reduced due to sequential metabolism (Pang and Gillette, 1979).

Intestinal PBPK models have been incorporated into whole body PBPK modeling. The semi-PBPK (SPBPK) model proposed by Hall and colleagues (Quinney et al., 2008; Zhang et al., 2009; Quinney et al., 2010) resembles the TM-PBPK and features the intestine and liver tissues separately while minimizing the number of other tissues involved, retaining characteristics of the intestine and liver to describe metabolism, transport and binding. The SPBPK model has been used to describe midazolam inhibition by intestinal and hepatically formed metabolites, N-desmethyldiltiazem from diltiazem in humans (Zhang et al., 2009) and hydroxyitraconazole from itraconazole in rats (Quinney et al., 2008), and in the estimation of the contribution of the intestine (~30 to 40%) in furamidine formation from pafuramidine in a prodrug-drug relationship in rats, then humans (Yan et al., 2012). Chow et al. (2011) used the combined TM-PBPK and SFM-PBPK models to predict the 1.8-fold and 2.6-fold induction of brain and kidney P-gp

protein expression with the vitamin D receptor ligand, 1α,25-dihydroxyvitamin D_3, respectively, and demonstrated a superior fit with the SFM-PBPK model in explaining the P-gp mediated excretion of digoxin. In the perfused rat intestine preparation in which the intestine is the only eliminating tissue, the SFM was found to be superior than the TM in describing morphine glucuronidation (Cong et al., 2000) and digoxin excretion by the P-glycoprotein under induced- and non-induced states (Liu et al., 2006). In this commentary, we appraised how these intestinal flow models differed by examining the effects of enterocytic flow on F_I and in turn, F_{sys} and the extents of intestinal and liver first-pass removal with use of simulations.

DMD Fast Forward. Published on June 27, 2012 as DOI: 10.1124/dmd.112.045872
This article has not been copyedited and formatted. The final version may differ from this version.

THEORETICAL: THE FLOW INTESTINAL MODELS

The TM and SFM. Historically, the TM and SFM were first compared by Cong et al. (2000) to offer an explanation of the higher extent of intestinal metabolism of erythromycin (Lown et al., 1995) and midazolam (Paine et al., 1996) in humans, and enalapril hydrolysis (Pang et al., 1985) and morphine glucuronidation in the vascularly perfused rat intestine preparation (Doherty and Pang, 2000) between oral (po) vs. intravenous (iv) dosing of drugs. Both models describe the effects of protein binding, enzymes for parallel and sequential pathways, and passive diffusion and/or transporter-driven permeation in metabolically- and transport-competent enterocytes (Cong et al., 2000). In this model, one or more metabolic pathways, denoted as the metabolic intrinsic clearances, $CL_{int,met1,I}$ and $CL_{int,met2,I}$, for the intestine, may exist for precursor drug, P, and similarly, $CL_{int,met1,H}$ and $CL_{int,met2,H}$ denote parallel metabolic pathways for the liver (Fig. 1). Drug secretion is represented by the $CL_{int,sec,I}$ for the intestinal secretion intrinsic clearance and $CL_{int,sec,H}$ for the liver biliary intrinsic clearance. Figure 1A denotes intestinal removal only, whereas Figure 1B, both intestinal and liver removal; there is no elimination from other organs and tissues, which are lumped as highly and poorly perfused tissues and blood. The influx and efflux clearances are denoted as CL_{d1}, CL_{d2}, CL_{d3} and CL_{d4} for the intestine (superscript I) and liver (superscript H); the unbound fractions in blood, intestine, and liver are denoted as f_B, f_I and f_H, respectively (though not shown in Fig. 1 for the sake of simplification). The single, significant difference between these models, TM and SFM, is the flow pattern for perfusion of tissue regions of the small intestine. The SFM emphasizes a small flow ($f_Q \approx$ 0.1-0.3x total intestinal flow) that perfuses the enterocyte region (en), and the remaining flow [$(1-f_Q)Q_{PV}$] is shunted to the serosal (s) or non-active region (Fig. 1). This segregated flow pattern contrasts with the TM that

DMD Fast Forward. Published on June 27, 2012 as DOI: 10.1124/dmd.112.045872
This article has not been copyedited and formatted. The final version may differ from this version.

describes the entire flow being able to reach the enterocyte or the total intestinal tissue (int), that is, $f_Q = 1$ (Cong et al., 2000).

Explicit solutions for the area under the curves (AUCs) for the TM- and SFM-PBPK models that feature the intestine as the only eliminating organ (Fig. 1A) were provided by Sun and Pang (2009; 2010). These AUCs could be further modified by consideration of protein binding (unbound fractions f_B and f_I) for po and iv dosing.

$$AUC_{po} = \frac{F_{abs} Dose_{po} CL^{I}_{d2}}{f_B CL^{I}_{d1}\left[CL_{int,met1,I} + CL_{int,met2,I} + (1-F_{abs}) CL_{int,sec,I} \right]} \quad (1)$$

and

$$AUC_{iv} = \frac{Dose_{iv}(f_Q Q_{PV} CL^{I}_{d2} + (f_B CL^{I}_{d1} + f_Q Q_{PV})\left[CL_{int,met1,I} + CL_{int,met2,I} + (1-F_{abs}) CL_{int,sec,I} \right]}{f_Q Q_{PV}\ f_B CL^{I}_{d1}\left[CL_{int,met1,I} + CL_{int,met2,I} + (1-F_{abs}) CL_{int,sec,I} \right]} \quad (2)$$

In the above equations, f_B is found to appear next to CL^{I}_{d1}. It is also recognized that tissue binding effects are non-operative since the f_I term cancels out in both the numerator and denominator. The difference in flow between the TM and SFM is denoted by f_Q, the fraction of Q_{PV} that perfuses the enterocyte region; for TM, $f_Q = 1$, whereas for SFM, $f_Q = 0.05$ to 0.3. The flow term is absent for AUC_{po} but present in AUC_{iv}.

Accordingly, the F_I and F_{sys} is,

$$\frac{AUC_{po}/Dose_{po}}{AUC_{iv}/Dose_{iv}} = F_{sys} = F_{abs} F_I = F_{abs} \frac{f_Q Q_{PV} CL^{I}_{d2}}{f_Q Q_{PV} CL^{I}_{d2} + (f_Q Q_{PV} + f_B CL^{I}_{d1})\left[CL_{int,met1,I} + CL_{int,met2,I} + (1-F_{abs}) CL_{int,sec,I} \right]} \quad (3)$$

Similarly, the AUCs for the TM- and SFM-PBPK models that feature both the intestine and liver as eliminating organs (Fig. 1B) have been solved (Sun and Pang 2010), and their ratio, after consideration given to protein binding, is,

DMD Fast Forward. Published on June 27, 2012 as DOI: 10.1124/dmd.112.045872
This article has not been copyedited and formatted. The final version may differ from this version.

$$\frac{AUC_{po}/Dose_{po}}{AUC_{iv}/Dose_{iv}} = F_{sys} = F_{abs}F_I F_H = F_{abs}\left[\frac{f_Q Q_{PV} CL^I_{d2}}{f_Q Q_{PV} CL^I_{d2} + (f_Q Q_{PV} + f_B CL^I_{d1})[CL^I_{int,met1} + CL^I_{int,met2} + CL^I_{int,sec}(1-F_{abs})]}\right]\left[\frac{Q_H(CL^H_{d2} + CL_{int,H})}{Q_H(CL^H_{d2} + CL_{int,H}) + f_B CL^H_{d1} CL_{int,H}}\right] \quad (4)$$

Again, tissue binding effects are non-operative since f_I and f_H, or the tissue unbound fractions for the intestine and liver, cancel out in both the numerator and denominator. In above equation, the f_B term appears next to the influx clearances for the intestine and liver, CL^I_{d1} and CL^H_{d1}. Increases in f_B would generally lower F_I according to Eqs. 3 and 4.

These solutions for F_I (Eqs. 3 and 4) revealed the blunting effect due to drug reabsorption, or the factor $(1-F_{abs})$, where F_{abs} is $k_a/(k_a+k_g)$ [where k_g is the luminal degradation constant that comprises of gastrointestinal transit and degradation] (Lin et al., 1999; Sun and Pang, 2009; Sun and Pang, 2010). The F_{abs} term has been reported to be highly correlated to the permeability of drug, P_{app} (Zhu et al., 2002; Corti et al., 2006; Kadono et al., 2010). Apical secretion mediated via the secretory intrinsic clearance, $CL_{int,sec,I}$, was nullified when the fraction absorbed ~1, rendering the conclusion that F_I is affected more by $CL_{int,met,I}$ and not so much by $CL_{int,sec,I}$ (Sun and Pang, 2009; Sun and Pang, 2010; Chow and Pang, 2012). As emphasized for the SFM, the partial flow suggests a bypass of enterocytes for drugs entering the intestinal tissue from the systemic circulation, whereas by design, drug given orally necessitates passage of the entire absorbed amount through the enterocyte region. This scenario would lead to a greater extent of intestinal removal for the drug given orally vs. when the drug is given intravenously (Cong et al., 2000), rendering "route-dependent intestinal removal".

The Q_{Gut} Model. Yang et al. (2007) constructed the "Q_{Gut} model" based on an effective flow, Q_{Gut}, to the enterocyte region, by relating this effective Q_{Gut} flow to the intestinal availability, F_I,

DMD Fast Forward. Published on June 27, 2012 as DOI: 10.1124/dmd.112.045872
This article has not been copyedited and formatted. The final version may differ from this version.

or F_G in their terminology. The equation for F_I or F_G is based analogously to the equation for hepatic availability (F_H), according to the well-stirred liver model (Pang and Rowland, 1977), where f_I is the unbound fraction of drug in intestinal tissue and $CL_{int,I}$, the total, intestinal intrinsic clearance that encompasses both secretion and metabolism.

$$F_I \text{ or } F_{Gut} = \frac{Q_{Gut}}{Q_{Gut} + f_I CL_{int,I}} \quad (5)$$

The effective flow, Q_{Gut}, is a hybrid term derived from the actual villous blood flow (Q_{villi}) [18 l/h or 300 ml/min (Gertz et al., 2010), representing ~48.4% of the total intestinal flow (assumed to equal the portal venous flow or Q_{PV}, ~ 620 ml/min) (Valentin, 2002; Yang et al., 2006; Yang et al., 2007)] and drug permeability clearance (CL_{perm}), a parameter that is normally estimated as the area x effective permeability (P_{eff}) assessed from perfused (human) jejunal studies, from Caco-2 cell apparent permeability (P_{app}), or based on physicochemical data such as hydrogen bond donors and polar surface area. The Q_{Gut} value of midazolam, a drug with high apparent permeability, was estimated to be 16.6 l/h, a value that is 92% of the value of Q_{villi} (Gertz et al., 2010).

$$Q_{Gut} = \frac{Q_{villi} CL_{perm}}{Q_{villi} + CL_{perm}} \quad (6)$$

For a drug that is highly permeable, $CL_{perm} >> Q_{villi}$, it may be deduced that $Q_{Gut} \cong Q_{villi}$.

Upon substitution of Eq. 6 into Eq. 5, one obtains

$$F_I \text{ or } F_{Gut} = \frac{\frac{Q_{villi} CL_{perm}}{Q_{villi} + CL_{perm}}}{\frac{Q_{villi} CL_{perm}}{Q_{villi} + CL_{perm}} + f_I CL_{int,I}} = \frac{Q_{villi} CL_{perm}}{Q_{villi} CL_{perm} + \left(Q_{villi} + CL_{perm}\right) f_I CL_{int,I}} \quad (7)$$

DMD Fast Forward. Published on June 27, 2012 as DOI: 10.1124/dmd.112.045872
This article has not been copyedited and formatted. The final version may differ from this version.

As originally conceived by Yang et al. (2007), the CL_{perm} term stands collectively for CL^{I}_{d1} and CL^{I}_{d2} but should be replaced appropriately by either CL^{I}_{d1} or CL^{I}_{d2}. Upon comparison of Eq. 7 with Eq. 3, the CL_{perm} terms for the Q_{Gut} model could now be assigned. By analogy to Eq. 3, it is further recognized that $f_I CL_{int,I}$ is equivalent to the composite term, $f_I[CLint_{,met1,I} + CL_{int,met2,I} + (1-F_{abs})CL_{int,sec,I})]$. The term, $f_I CL_{int,I}$ that represents the summed unbound metabolic and secretory intrinsic clearances, fails to consider the intestinal secretion followed by reabsorption of the secreted material in the lumen. Upon consideration of all these missed events,

$$F_I \text{ or } F_{Gut} = \frac{Q_{villi} CL_{perm}}{Q_{villi} CL_{perm} + \left(Q_{villi} + CL_{perm}\right) f_I CL_{int,I}}$$

$$\text{or } \frac{Q_{villi} CL^{I}_{d2}}{Q_{villi} CL^{I}_{d2} + \left(Q_{villi} + f_B CL^{I}_{d1}\right)\left[CL_{int,met1,I} + CL_{int,met2,I} + (1-F_{abs})CL_{int,sec,I}\right]} \quad (8)$$

one obtains Eq. 8 for the Q_{Gut} model that appears in an equivalent format as that for the TM and SFM (Eq. 3). One sees similarities between the SFM/TM and the Q_{Gut} model. The $f_Q Q_{PV}$ term for the SFM is equivalent to the Q_{villi} term of the Q_{Gut} model (300 ml/min), which describes a partial flow (f_Q = 0.484) perfusing the enterocyte region.

DMD Fast Forward. Published on June 27, 2012 as DOI: 10.1124/dmd.112.045872
This article has not been copyedited and formatted. The final version may differ from this version.

RESULTS

Comparison of f_Q. A proper comparison of these models has not been made in any rigorous fashion, especially in regard to f_Q on F_I. The starting point of the comparison is f_Q, being of a low value (~0.1 to 0.3) for the SFM, ~0.5 (Q_{villi}/Q_{PV} = 0.484) for the Q_{Gut} model, and high (1.0) for the TM. We felt that the f_Q term could serve as an important variable for selection of the most appropriate model to best describe the intestine. Upon perusal of the literature, estimates of Q_{Gut} according to Eq. 2 for various drugs varied from 2.4, 5.7, 8.6 to 16.6 l/h, corresponding to 6.5 to 43% of the total intestinal flow, with good predictions for midazolam but poor estimation of F_I (or F_G) for saquinavir *in vivo* (Gertz et al., 2010). Some of these f_Q values for the Q_{Gut} model were higher than the f_Q values of 0.07, 0.024, and 0.2 estimated from fits of the SFM to the data on benzoic acid (Cong et al., 2001), morphine (Cong et al., 2000) and digoxin (Liu et al., 2006), respectively, from vascularly perfused rat small intestine preparations. For digoxin, which is mainly excreted unchanged in the mouse *in vivo*, a value of 0.16 was found for f_Q (Chow et al., 2011). The f_Q terms, whether for the SFM or for Q_{Gut} model, were both less than unity (Gertz et al., 2010; Chow and Pang, 2012), with f_Q values being higher than 0.3 for the Q_{Gut} model. Values of f_Q for the SFM were lower and corresponded better with published evidence that suggests segregated flows for the small intestine, and that a small fraction of flow (5-30%) perfuses the active, mucosal region (Granger et al., 1980).

Simulation of F_I. Eq. 1 for the TM and SFM which considers the intestine as the only eliminating organ, lacks any of the flow terms and suggests that AUC_{po} is identical among the TM, Q_{Gut} model, and SFM, whereas the AUC_{iv} intended for the TM/SFM (Eq. 2) consisted of the flow term, $f_Q Q_{PV}$ for SFM and TM, and Q_{villi} for the Q_{Gut} model, by analogy. Thus, different AUC_{iv} values for the Q_{Gut} model and the SFM resulted when the flow term was replaced by the

DMD Fast Forward. Published on June 27, 2012 as DOI: 10.1124/dmd.112.045872
This article has not been copyedited and formatted. The final version may differ from this version.

appropriate flow rate, $f_Q Q_{PV}$ or Q_{villi}. Since the rate of intestinal metabolism is dependent on the flow rate for delivery of substrate, it may be concluded that, when a smaller flow reaches the enterocyte region, a smaller intestinal removal rate results with systemic delivery, supplying a ranking of the intestinal removal rate as SFM < Q_{Gut} model < TM after intravenous dosing. The lower flow rate stipulated by the SFM in bringing the substrate into enterocyte region yielded a higher AUC_{iv} (ranking for AUC_{iv}: SFM > Q_{Gut} model > TM) and consequently a lower F_I for the SFM compared to the Q_{Gut} model and TM for given $CL_{int,met,I}$ values. This view was supported by the simulations (Fig. 2A). The ranking of F_I was SFM < Q_{Gut} model < TM.

It was further observed that the expressions for the F_I terms were identical for the scenario in which the intestine is the only eliminating organ (Eq. 3) and when the intestine and liver are both eliminating organs (Eq. 4). These patterns for F_I (Fig. 2A) were translated into F_{sys} for any given F_H (= 0.1, 0.5 or 0.9, Fig. 2B). Again, the simulated patterns are consistent with the view that a decreased intestinal extraction ratio is accompanied an increase in mesenteric flow (Chen and Pang, 1997; Chalasani et al., 2001; Yang et al., 2007; Chow and Pang, 2012); the lower intestinal removal rate due to lower intestinal flows would result in a higher hepatic processing, as observed experimentally by Chen and Pang (1997).

Changing CL'_{d1} or CL'_{d2} on F_I. When we further examined effects of the basolateral influx (CL'_{d1}) or efflux (CL'_{d2}) transport clearances for drugs that exhibit varying degrees of absorption (described by F_{abs} = 0.1, 0.5 and 1.0), all models showed that F_I was attenuated when CL'_{d1} was increased or when CL'_{d2} was decreased (Fig. 3). Increasing the influx basolateral clearance (CL'_{d1}) from low to high (left column from 1x to 5x and 20x blood flow, Fig. 3) would lead to lower F_I values, whereas upon increasing values of CL'_{d2} from low to higher values (from 1x to 5x flow, middle column, then 20x flow, right column, Fig. 3), higher F_I were attained due to ability of the

influxed drug to escape intestinal enzymes intracellularly. The f_Q effects from the flow models were apparent again with the simulations, and the ranking for F_I values was SFM < Q_{Gut} model < TM (Fig. 3).

Contributions from Intestine and Liver to First-Pass Effect. To assess the contributions from the intestine vs. the liver in first-pass removal among these flow-intestinal models, we further simulated the rates predicted from the mass equations shown below (Eqs. 9 and 10) that described the rates of intestinal (v_I) and hepatic (v_H) removal. For estimation of the rates, there exists the need to define the flow-averaged portal venous concentration, $\overline{C}_{PV}$, to account for the partial flow entering the enterocyte region and for accurate prediction of the intestinal removal rate, v_I.

$$\overline{C}_{PV} = \frac{f_Q Q_{PV} F_I C_A + (1-f_Q) Q_{PV} C_A}{Q_{PV}} = C_A \left[f_Q F_I + (1-f_Q) \right] \quad (9)$$

$$v_I = Q_{PV} C_A - Q_{PV} \overline{C}_{PV} = Q_{PV} C_A \left\langle 1 - [f_Q F_I + (1-f_Q)] \right\rangle = f_Q Q_{PV} C_A (1-F_I) \quad (10)$$

and

$$v_H = Q_{PV} \overline{C}_{PV} E_H + Q_{HA} C_A E_H = C_A E_H \left\langle Q_{PV} [f_Q F_I + (1-f_Q)] + Q_{HA} \right\rangle \quad (11)$$

Here, E is the extraction ratio for the intestine or liver that equals (1-F), and C_A is the arterial concentration. The fractional contributions by the intestine and liver were then calculated.

The fractional contribution by intestine to the first-pass effect is

$$= \frac{v_I}{v_I + v_H} = \frac{f_Q Q_{PV} (1-F_I)}{f_Q Q_{PV} (1-F_I) + E_H \left\langle Q_{PV} [f_Q F_I + (1-f_Q)] + Q_{HA} \right\rangle} \quad (12)$$

DMD Fast Forward. Published on June 27, 2012 as DOI: 10.1124/dmd.112.045872
This article has not been copyedited and formatted. The final version may differ from this version.

and the fractional contribution by liver to the first-pass effect is

$$= \frac{v_H}{v_I + v_H} = \frac{E_H \langle Q_{PV}[f_Q F_I + (1 - f_Q)] + Q_{HA} \rangle}{f_Q Q_{PV}(1-F_I) + E_H \langle Q_{PV}[f_Q F_I + (1 - f_Q)] + Q_{HA} \rangle} \quad (13)$$

Q_{villi} replaces $f_Q Q_{PV,}$ in Eqs. 9, 10, 12, and 13 for the Q_{Gut} model, with f_Q = 0.484. Again, substitution of f_Q (=1, 0.484 and 0.1, respectively, for TM, Q_{Gut} model and SFM) embedded in F_I or E_I (Eq. 3) yielded the corresponding fractional removal estimates. Accordingly, the lower intestinal removal rate (v_I) predicted by the SFM due to the reduced flow rate resulted in a correspondingly higher contribution by the liver due to the substrate sparing effect of the intestine (Fig. 4). Whereas for TM, the greater intestinal contribution in removing the drug led to a lesser removal contribution by the liver due to a substrate depleting effect of the intestine (Fig. 4). Predictions from the Q_{Gut} model on the intestinal and liver contributions to first-pass removal fell in between those for the SFM and TM, and the patterns were similar when F_{abs} = 0.1 or 0.9 (Fig. 4).

Again, the predictions revealed that the f_Q values in different intestinal models affected the contributions of the intestine and liver in the first-pass effect. For any given $CL_{int,met1,I}$, this difference translates to ranking for the intestinal contribution to the first-pass effect as TM > Q_{Gut} > SFM, and for the liver, the ranking is TM < Q_{Gut} < SFM. These opposite trends in intestinal vs. hepatic contributions to first-pass have been discussed by Xu et al. (1989) and Chen and Pang (1997), attributing their observations to the anterior positioning of the intestine without recognizing the segregated flow effects. It must be commented that the value of F_{abs} was not very apparent to affect the contributions of the intestine or liver in first-pass removal in these simulations; the F_{abs} term affected only the reabsorption of the intestinally secreted drug (Eqs. 3

DMD Fast Forward. Published on June 27, 2012 as DOI: 10.1124/dmd.112.045872
This article has not been copyedited and formatted. The final version may differ from this version.

and 4), which was, for all intent and purpose, a minor pathway ($CL_{int,sec,I}$ was set as 200 ml/min) relative to values of $CL_{int,met1,I}$ examined.

Effects of Binding

The mathematical manipulation revealed that tissue binding effects are non-operative since the unbound fraction terms in intestine (f_I) or liver (f_H) canceled out in both the numerator and denominator. As seen from Eqs. 3 and 4, only the f_B term persisted in the equations and was associated with the influx clearances, CL_{d1}, for the intestine and liver (superscripted I and H, respectively). Upon changing f_B at three sets of $CL_{int,met1,I}$ values for the various models (Fig. 5), it could be seen that increased values of f_B generally lowered F_I (Fig. 5). Exceedingly similar patterns were observed for F_{abs} = 0.1 and 0.9.

DMD Fast Forward. Published on June 27, 2012 as DOI: 10.1124/dmd.112.045872
This article has not been copyedited and formatted. The final version may differ from this version.

DISCUSSION

This examination reveals that f_Q is the key issue in the prediction of F_I and contribution of both the intestine and liver to first-pass removal. The Q_{Gut} model is similar to the SFM in many respects, except that a higher limit exists for f_Q. The simulations, based on the various f_Q values, show that the predicted intestinal availability of the Q_{Gut} model falls between those of the TM and SFM models under varying conditions of efflux and influx clearances (Fig. 3). Decreased intestinal availabilities are expected with lower f_Q values (Fig. 2), and this contributes to a greater proportion of first-pass extraction by the liver, the posterior organ (Fig. 4).

A major issue for the prediction of F_I is the choice of the correct f_Q value for intestinal models, especially for the Q_{Gut} model. The problem, that the intended Q_{Gut} term is a hybrid function of Q_{villi} and CL_{perm} (as shown in Eq. 7), could now be circumvented with use of Eq. 8. Although literature reports for the Q_{Gut} model suggest that f_Q varies between 0.07 and 0.43, we suggest use of the unambiguous Q_{villi} term or $f_Q Q_{PV}$ (f_Q = 0.484) for the Q_{Gut} model, with inclusion of the CL^{I}_{d1} and CL^{I}_{d2} terms in lieu of CL_{perm}, in a format similar to those for the SFM and TM (Eq. 8) to define to the fractional flow and the transport intrinsic clearances. This revelation implies that the effective flow rate to the enterocyte region (f_Q = 0.484) for the Q_{Gut} model is higher than that for the SFM. Another revelation is that $f_I CL_{int,I}$ in Q_{Gut} model falls short of the more comprehensive term, $[CL_{int,met,I} + (1\text{-}F_{abs})CL_{int,sec,I}]$, in the prediction of F_G (or F_I in our terms). This may be another reason why poor prediction prevails for some drugs that are P-gp substrates (Gertz et al., 2010). Indeed, improved estimation of P_{eff} with use of a P-gp inhibitor seemed to improve the F_I prediction of saquinavir (Gertz et al., 2011). The need for f_I in the equation for the Q_{Gut} model is questionable since the term cancels out even when the binding effects of intestinal tissue on efflux, metabolism or excretion are taken into consideration.

Other theoretical modeling that considers heterogeneity of transporters and enzymes along the length of the small intestine, as in the segmental traditional (STM) and segmental segregated flow (SSFM) models (counterparts of TM and SFM), has revealed that metabolic heterogeneity strongly impacts F_I (Tam et al., 2003). Wu (2011) has recently commented, in a theoretical examination, that heterogeneity matters in predicting F_{sys} after comparison of simulations from the TM-PBPK and SSFM-PBPK models on the systemic availability of the parent aglycone during the process of enterohepatic circulation of biliarily excreted glucuronides. The consideration of heterogeneity of transporters and enzymes on intestinal modeling *in vivo* surfaced much later, possibly due to the difficulty in obtaining population and length-averaged estimates on physiological dimensions of the lumen, surface area, flow, and enzymes and transporters in humans and animals (Badhan et al., 2009; Bruyère et al., 2010). Other compartmental models, when coupled with a refined description on the linear transfer kinetics of state properties of the drug (unreleased or solid form, undissolved or aggregate form, and dissolved or solution form), physicochemical properties (pKa, solubility, particle size, particle density, and permeability), physiological properties (gastric emptying, intestinal transit rate, intestinal metabolism, and luminal transport), and dosage factors (dosage form and dose) in the GIT, show much improved predictions of drug kinetics (Agoram et al., 2001; Hendriksen et al., 2003), especially with inclusion of heterogeneity factors in the modeling (Bolger et al., 2009; Abuasal et al., 2012). The ability of many of the present models to fully describe metabolite kinetics, however, remains uncertain. We have noted that heterogeneity models such as the SSFM and STM (Tam et al., 2003), whether necessary or not, are more pertinent in cases of enzyme heterogeneity among the segments. In absence of metabolism by the intestine, we found that the STM and SSFM perform equally well as the TM and SFM, as found for studies on the

absorption of benzoic acid (Cong et al., 2001) and digoxin absorption and efflux by P-gp (Liu et al., 2006) in the vascularly perfused intestine preparation. The presence of metabolite data is an absolutely necessity for the discrimination between the SFM and TM.

It can be concluded that the designated flow rate to the enterocyte region of the intestine, defined according to the different intestinal flow models, strongly impacts F_I and F_{sys}, and the proportions of intestinal and liver in first-pass removal. With the solved equations for the AUCs, it is apparent that predictions on the interplay between intestine and hepatic transporters and enzymes are readily attainable (Pang et al., 2009; Sun and Pang, 2010). Key issues for proper intestinal modeling are the accurate definition of f_Q and improved estimates of the transport clearances. The proper definition of f_Q is of paramount importance and this awaits use of sophisticated tools to properly estimate the enteroctye vs. the total intestinal flow rate. Notwithstanding the deficiencies persisting in all of the mentioned models, it is rewarding to see how the theoretical refinement in intestinal modeling has advanced our activity and knowledge towards how transporter- and enzyme heterogeneity as well as segregated flow patterns affect drug metabolism and excretion by the small intestine and liver in first-pass removal during oral drug absorption.

DMD Fast Forward. Published on June 27, 2012 as DOI: 10.1124/dmd.112.045872
This article has not been copyedited and formatted. The final version may differ from this version.

AUTHORSHIP CONTRIBUTIONS

Participated in research design: Pang, K.S. and Chow, E.C.
Conducted experiments: Chow, E.C. Pang, K.S.
Performed data analysis: Chow, E.C. Pang, K.S.
Wrote or contributed to the writing of the manuscript: Pang, K.S. and Chow, E.C.

References

Abuasal BS, Bolger MB, Walker DK, and Kaddoumi A (2012) In silico modeling for the nonlinear absorption kinetics of UK-343,664: a P-gp and CYP3A4 substrate. *Mol Pharm* **9**: 492-504.

Agoram B, Woltosz WS, and Bolger MB (2001) Predicting the impact of physiological and biochemical processes on oral drug bioavailability. *Adv Drug Deliv Rev* **50**(Suppl 1):S41-S67.

Badhan R, Penny J, Galetin A, and Houston JB (2009) Methodology for development of a physiological model incorporating CYP3A and P-glycoprotein for the prediction of intestinal drug absorption. *J Pharm Sci* **98:**2180-2197.

Bolger MB, Lukacova V, and Woltosz WS (2009) Simulations of the nonlinear dose dependence for substrates of influx and efflux transporters in the human intestine. *AAPS J* **11**:353-363.

Bruyère A, Declèves X, Bouzom F, Ball K, Marques C, Treton X, Pocard M, Valleur P, Bouhnik Y, Panis Y, Scherrmann JM, and Mouly S (2010) Effect of variations in the amounts of P-glycoprotein (ABCB1), BCRP (ABCG2) and CYP3A4 along the human small intestine on PBPK models for predicting intestinal first pass. *Mol Pharm* **7:**1596–1607.

Chalasani N, Gorski JC, Patel NH, Hall SD, and Galinsky RE (2001) Hepatic and intestinal cytochrome P450 3A activity in cirrhosis: effects of transjugular intrahepatic portosystemic shunts. *Hepatology* **34:**1103-1108.

Chen J and Pang KS (1997) Effect of flow on first-pass metabolism of drugs: single pass studies on 4-methylumbelliferone conjugation in the serially perfused rat intestine and liver preparations. *J Pharmacol Exp Ther* **280:**24-31.

Chow EC and Pang KS (2013) Why we need PBPK modeling to examine intestine and liver oral drug absorption. *Curr Drug Metab* accepted

Chow EC, Durk MR, Cummins CL, and Pang KS (2011) 1α,25-Dihydroxyvitamin D_3 up-regulates P-glycoprotein via the vitamin D receptor and not farnesoid X receptor in both *fxr(-/-)* and *fxr(+/+)* mice and increased renal and brain efflux of digoxin in mice *in vivo*. *J Pharmacol Exp Ther* **337:**846-859.

Cong D, Doherty M, and Pang KS (2000) A new physiologically based, segregated-flow model to explain route-dependent intestinal metabolism. *Drug Metab Dispos* **28:**224-235.

Cong D, Fong AK, Lee R, and Pang KS (2001) Absorption of benzoic acid in segmental regions of the vascularly perfused rat small intestine preparation. *Drug Metab Dispos* **29:**1539-1547.

Corti G, Maestrelli F, Cirri M, Furlanetto S, and Mura P (2006) Development and evaluation of an in vitro method for prediction of human drug absorption I. Assessment of artificial membrane composition. *Eur Pharm Sci* **27**:346-353.

Darwich AS, Neuhoff S, Jamei M, and Rostami-Hodjegan A (2010) Interplay of metabolism and transport in determining oral drug absorption and gut wall metabolism: a simulation assessment using the "Advanced Dissolution, Absorption, Metabolism (ADAM)" model. *Curr Drug Metab* **11:**716-729.

de Lannoy IA and Pang KS (1986) Presence of a diffusional barrier on metabolite kinetics: enalaprilat as a generated versus preformed metabolite. *Drug Metab Dispos* **14:**513-520.

de Lannoy IA and Pang KS (1987) Effect of diffusional barriers on drug and metabolite kinetics. *Drug Metab Dispos* **15:**51-58.

Doherty MM and Pang KS (2000) Route-dependent metabolism of morphine in the vascularly perfused rat small intestine preparation. *Pharm Res* **17:**291-298.

Eeckhoudt SL, Horsmans Y, and Verbeeck RK (2002) Differential induction of midazolam metabolism in the small intestine and liver by oral and intravenous dexamethasone pretreatment in rat. *Xenobiotica* **32:**975-984.

Fan J, Chen S, Chow EC, and Pang KS (2010) PBPK modeling of intestinal and liver enzymes and transporters in drug absorption and sequential metabolism. *Curr Drug Metab* **11:**743-761.

Fang C and Zhang QY (2010) The role of small-intestinal P450 enzymes in protection against systemic exposure of orally administered benzo[a]pyrene. *J Pharmacol Exp Ther* **334:**156-163.

Fromm MF, Busse D, Kroemer HK, and Eichelbaum M (1996) Differential induction of prehepatic and hepatic metabolism of verapamil by rifampin. *Hepatology* **24:**796-801.

Galetin A, Gertz M, and Houston JB (2010) Contribution of intestinal cytochrome P450-mediated metabolism to drug-drug inhibition and induction interactions. *Drug Metab Pharmacokinet* **25:**28-47.

Gertz M, Harrison A, Houston JB, and Galetin A (2010) Prediction of human intestinal first-pass metabolism of 25 CYP3A substrates from *in vitro* clearance and permeability data. *Drug Metab Dispos* **38:**1147-1158.

Gertz M, Houston JB, and Galetin A (2011) Physiologically based pharmacokinetic modeling of intestinal first-pass metabolism of CYP3A substrates with high intestinal extraction. *Drug Metab Dispos* **39:**1633-1642

Granger DN, Richardson PD, Kvietys PR, and Mortillaro NA (1980) Intestinal blood flow. *Gastroenterology* **78:**837-863.

Hendriksen BA.; Felix, M.V. and Bolger, M.B. (2003) The composite solubility versus pH profile and its role in intestinal absorption prediction. *AAPS PharmSci* **5**(1), E4.

Kadono K, Akabane T, Tabata K, Gato K, Terashita S, and Teramura T (2010) Quantitative prediction of intestinal metabolism in humans from a simplified intestinal availability model and empirical scaling factor. *Drug Metab Dispos* **38**:1230-1237.

Lin JH, Chiba M and, Baillie TA (1999) Is the role of the small intestine in first-pass metabolism overemphasized? *Pharmacol Rev* **51:**135-158.

Liu S, Tam D, Chen X, and Pang KS (2006) P-Glycoprotein and an unstirred water layer barring digoxin absorption in the vascularly perfused rat small intestine preparation: induction studies with pregnenolone-16α-carbonitrile. *Drug Metab Dispos* **34:**1468-1479.

Liu YT, Hao HP, Xie HG, Lai L, Wang Q, Liu CX, and Wang GJ (2010) Extensive intestinal first-pass elimination and predominant hepatic distribution of berberine explain its low plasma levels in rats. *Drug Metab Dispos* **38:**1779-1784.

Lledó-García R, Nácher A, Casabó VG, and Merino-Sanjuán M (2011) A pharmacokinetic model for evaluating the impact of hepatic and intestinal first-pass loss of saquinavir in the rat. *Drug Metab Dispos* **39**:294-301.

Lown KS, Thummel KE, Benedict PE, Shen DD, Turgeon DK, Berent S, and Watkins PB (1995) The erythromycin breath test predicts the clearance of midazolam. *Clin Pharmacol Ther* **57:**16-24.

Mouly S, Lown KS, Kornhauser D, Joseph JL, Fiske WD, Benedek IH, and Watkins PB (2002) Hepatic but not intestinal CYP3A4 displays dose-dependent induction by efavirenz in humans. *Clin Pharmacol Ther* **72:**1-9.

Paine MF, Shen DD, Kunze KL, Perkins JD, Marsh CL, McVicar JP, Barr DM, Gillies BS, and Thummel KE (1996) First-pass metabolism of midazolam by the human intestine. *Clin Pharmacol Ther* **60:**14-24.

Pang KS (2003) Modeling of intestinal drug absorption: roles of transporters and metabolic enzymes (for the Gillette Review Series). *Drug Metab Dispos* **31:**1507-1519.

Pang KS and Durk MR (2010) Physiologically-based pharmacokinetic modeling for absorption, transport, metabolism and excretion. *J Pharmacokinet Biopharm* **37:**591-615.

Pang KS and Gillette JR (1979) Sequential first-pass elimination of a metabolite derived from a precursor. *J Pharmacokinet Biopharm* **7:**275-290.

Pang KS, Cherry WF, and Ulm EH (1985) Disposition of enalapril in the perfused rat intestine liver preparation: absorption, metabolism and first pass effect. *J Pharmacol Exp Ther* **233:**788–795.

Pang KS, Maeng HJ, and Fan J (2009) Interplay of transporters and enzymes in drug and metabolite processing. *Mol Pharm* **6:**1734-1755.

Pang KS, Morris ME, and Sun H (2008) Formed and preformed metabolites: facts and comparisons. *J Pharm Pharmacol* **60:**1247-1275.

Pang KS and Rowland M (1977) Hepatic clearance of drugs. I. Theoretical considerations of a "well-stirred" model and a "parallel tube" model. Influence of hepatic blood flow, plasma and blood cell binding, and the hepatocellular enzymatic activity on hepatic drug clearance. *J Pharmacokinet Biopharm* **5:**625-653.

Quinney SK, Galinsky RE, Jiyamapa-Serna VA, Chen Y, Hamman MA, Hall SD, and Kimura RE (2008) Hydroxyitraconazole, formed during intestinal first-pass metabolism of

itraconazole, controls the time course of hepatic CYP3A inhibition and the bioavailability of itraconazole in rats. *Drug Metab Dispos* **36:**1097-1101.

Quinney SK, Zhang X, Lucksiri A, Gorski JC, Li L, and Hall SD (2010) Physiologically based pharmacokinetic model of mechanism-based inhibition of CYP3A by clarithromycin. *Drug Metab Dispos* **38:**241-248.

Rowland Yeo K, Jamei M, Yang J, Tucker GT, and Rostami-Hodjegan A (2010) Physiologically based mechanistic modelling to predict complex drug-drug interactions involving simultaneous competitive and time-dependent enzyme inhibition by parent compound and its metabolite in both liver and gut - the effect of diltiazem on the time-course of exposure to triazolam. *Eur J Pharm Sci* **39:**298-309.

Sun H and Pang KS (2009) Disparity in intestine disposition between formed and preformed metabolites and implications: a theoretical study. *Drug Metab Dispos* **37:**187-202.

Sun H and Pang KS (2010) Physiological modeling to understand the impact of enzymes and transporters on drug and metabolite data and bioavailability estimates. *Pharm Res* **27:**1237-1254.

Suzuki H and Sugiyama Y (2000a) Role of metabolic enzymes and efflux transporters in the absorption of drugs from the small intestine. *Eur J Pharm Sci* **12:**3-12.

Suzuki H and Sugiyama Y (2000b) Transport of drugs across the hepatic sinusoidal membrane: sinusoidal drug influx and efflux in the liver. *Semin Liver Dis* **20:**251-263.

Tam D, Tirona RG, and Pang KS (2003) Segmental intestinal transporters and metabolic enzymes on intestinal drug absorption. *Drug Metab Dispos* **31:**373-383.

Thummel KE, O'Shea D, Paine MF, Shen DD, Kunze KL, Perkins JD, and Wilkinson GR (1996) Oral first-pass elimination of midazolam involves both gastrointestinal and hepatic CYP3A-mediated metabolism. *Clin Pharmacol Ther* **59**:491-502.

Valentin J (2002) In, *Basic Anatomical and Physiological Data for Use in Radiological Protection: Reference Value*s. Pergamon, Oxford.

Wu B (2011) Use of physiologically based pharmacokinetic models to evaluate the impact of intestinal glucuronide hydrolysis on the pharmacokinetics of aglycone. *J Pharm Sci* **101**:1281-1301.

Xu X, Hirayama H, and Pang KS (1989) First-pass metabolism of salicylamide. Studies in the once-through vascularly perfused rat intestine-liver preparation. *Drug Metab Dispos* **17:**556-563.

Yan GZ, Generaux CN, Yoon M, Goldsmith RB, Tidwell RR, Hall JE, Olson CA, Clewell HJ, Brouwer KL, and Paine MF (2012) A semiphysiologically based pharmacokinetic modeling approach to predict the dose-exposure relationship of an antiparasitic prodrug/active metabolite pair. *Drug Metab Dispos* **40:**6-17.

Yang J, Jamei M, Heydari A, Yeo KR, de la Torre R, Farré M, Tucker GT and Rostami-Hodjegan A (2006) Implications of mechanism-based inhibition of CYP2D6 for the pharmacokinetics and toxicity of MDMA. *J Psychopharmacol* **20:**842-849.

Yang J, Jamei M, Yeo KR, Tucker GT and Rostami-Hodjegan A (2007) Prediction of intestinal first-pass drug metabolism. *Curr Drug Metab* **8:**676-684.

Zhang X, Quinney SK, Gorski JC, Jones DR and Hall SD (2009) Semiphysiologically based pharmacokinetic models for the inhibition of midazolam clearance by diltiazem and its major metabolite. *Drug Metab Dispos* **37:**1587-1597.

Zhu Y, D'Agostino J and Zhang QY (2011) Role of intestinal cytochrome P450 (P450) in modulating the bioavailability of oral lovastatin: insights from studies on the intestinal epithelium-specific P450 reductase knockout mouse. *Drug Metab Dispos* **39**:939-943.

Zhu C, Jiang L, Chen TM and Hwang KK (2002) A comparative study of artificial membrane permeability assay for high throughput profiling of drug absorption potential. *Eur J Med Chem* **37**: 399-407.

FOOTNOTES

This work was supported by the Canadian Institute for Health Research, CIHR (K.S.P.) and the Alexander Graham Bell NSERC fellowship, National Science and Engineering Research Council of Canada, NSERC (E.C.C.)

DMD Fast Forward. Published on June 27, 2012 as DOI: 10.1124/dmd.112.045872
This article has not been copyedited and formatted. The final version may differ from this version.

Legends

Figure 1. **Whole body PBPK, with the liver and other lumped compartments (highly perfused, poorly perfused) being connected to the intestine model (TM and SFM), depicting the intestine (A) and intestine and liver (B) as the eliminating tissue(s)/organs (s)**. The intestine subcompartments are: for TM, subscripts int and intB denote intestinal tissue and intestinal blood, respectively; for SFM, subscripts en and enB denote enterocyte and enterocyte blood, respectively; s and sB denote serosal tissue and serosal blood, respectively. For the liver, subscripts L and LB represent liver tissue and liver blood, respectively; subscript R denotes the reservoir or blood compartment. For TM, the intestine represents a well-mixed enterocyte region and receives the entire intestinal blood flow, Q_I or Q_{PV}. For SFM, the blood flow is segregated to perfuse the enterocyte and serosal regions; the flow to the enterocyte region is denoted as $f_Q Q_{PV}$, and the serosal region, $(1-f_Q)Q_{PV}$. At the basolateral membrane, the drug influx and efflux clearances into or out of the intestine or enterocyte are characterized by the transport clearance parameters, CL^I_{d1} and CL^I_{d2} respectively. For SFM, additional influx and efflux clearance into or out of the serosal tissue compartment are characterized by the transport clearance parameters, CL^I_{d3} and CL^I_{d4}. The liver receives blood from hepatic blood artery (Q_{HA}) arising from the blood compartment and venous flow, Q_{PV}, from the intestine; the summed blood flow exits the liver as Q_H. The influx and efflux clearances of the drug into or out of the liver are CL^H_{d1} and CL^H_{d2}, respectively. Intrinsic metabolic clearance of parent drug (P) to form the primary metabolites in the intestine are denoted as $CL_{int,met1,I}$ and $CL_{int,met2,I}$ and those in liver are $CL_{int,met1,H}$ and $CL_{int,met2,H}$; the intestine and liver secrete P out via secretory intrinsic clearances, $CL_{int,sec,I}$ and $CL_{int,sec,H}$, respectively. The bile flow rate is denoted as Q_{bile}. Drug administrated orally (solution form) is administered into the lumen, and may be either absorbed into intestine with the rate constant, k_a, or degraded in lumen by the rate constant, k_g; drug given intravenously directly enters the blood compartment.

Figure 2 **Effects of changing $CL_{int,met1,I}$ (e.g. induction or inhibition of enzymes) on F_I according to the TM, Q_{Gut} model and SFM with Eq. 4 (A) and F_{sys} with the F_I values shown in (A) under varying conditions of F_H = 0,1, 0.5 and 0.9 (B)**. In this simulation, $CL_{int,sec,I}$ was set as 200 ml/min; Q_{PV} = 620 ml/min; f_Q = 1.0 (TM), or 0.484 (Q_{Gut} model) and 0.1 (SFM); F_{abs} = 0.1, 0.5, or 0.9; $CL_{int,met2,I}$ = 0; CL^I_{d1} = CL^I_{d2} = 20x Q_{PV}, denoting a highly permeable drug.

Figure 3. **Effects of varying basolateral transport clearances, CL^I_{d1} and CL^I_{d2}, on F_I according to Eq. 3, for drugs which are highly absorbed (F_{abs} = 0.9)**. For these simulations, $CL_{int,sec,I}$ was set as 200 ml/min; Q_{PV} was set as 620 ml/min, and f_Q = 1.0 (for TM), or 0.484 (for Q_{Gut} model) and 0.1 (for SFM). Values of CL^I_{d1} and CL^I_{d2} were altered from 1x, 5x, and 20x Q_{PV}. The value of $CL_{int,met2,I}$, the intrinsic clearance for the alternate metabolic pathway, was set as 0.

DMD Fast Forward. Published on June 27, 2012 as DOI: 10.1124/dmd.112.045872
This article has not been copyedited and formatted. The final version may differ from this version.

Figure 4. **Simulation for the fractional contributions of the intestine, $\frac{V_I}{V_I+V_H}$ (Eq. 12) (A) and liver, $\frac{V_H}{V_I+V_H}$ (Eq. 13), (B).** The designated drug examples vary from being poorly to highly absorbed (F_{abs} = 0.1and 0.9), whose hepatic availability (F_H) vary from 0.1 to 0.9, Q_{HA} = 300 ml/min and CL^I_{d1} = CL^I_{d2} = 20x Q_{PV}, with an excretion component $CL_{int,sec,I}$ = 200 ml/min and a non-existent, alternate metabolic pathway ($CL_{int,met2,,I}$ = 0); the assigned flow rates were: Q_{PV} = 620 ml/min; f_Q = 1.0 (TM) or 0.1 (or Q_{en}/Q_{PV} for SFM). Simulations for the Q_{Gut} model (f_Q = 0.484) were intermediate of those for the SFM and TM. See text for details.

Figure 5. **Effects of changing f_B on F_I according to the TM, Q_{Gut} model and SFM with Eq. 3 at F_{abs} = 0. 1 (A) or 0.9 (B) at $CL_{int,met1,I}$ = 100, 1000, or 2000 ml/min**. In this simulation, $CL_{int,sec,I}$ was set as 200 ml/min; Q_{PV} = 620 ml/min; f_Q = 1.0 (TM), 0.484 (Q_{Gut} model) or 0.1 (SFM); $CL_{int,met2,I}$ = 0; CL^I_{d1} = CL^I_{d2} = 20x Q_{PV}, denoting a highly permeable drug. See text for details.

Figure 1

(A)

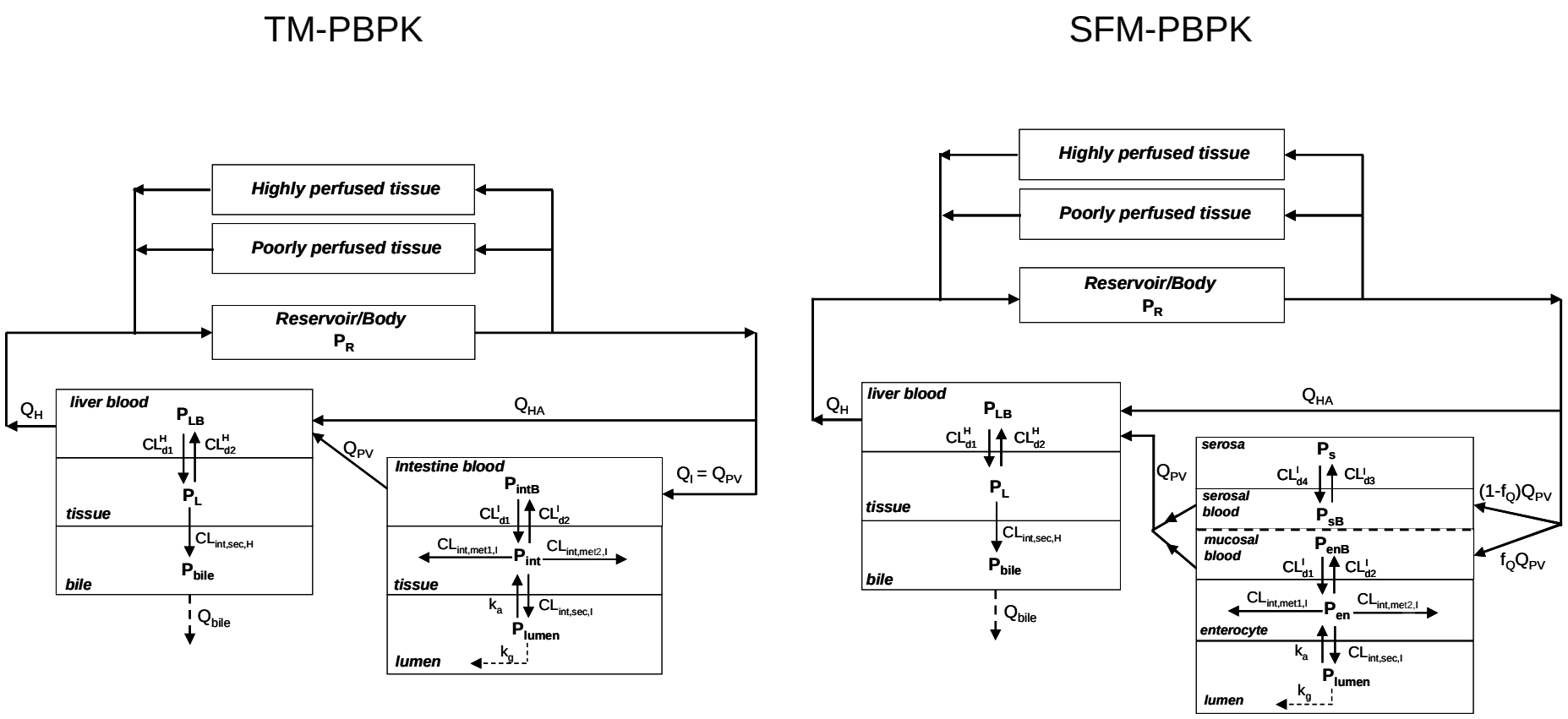

Figure 1

(B)

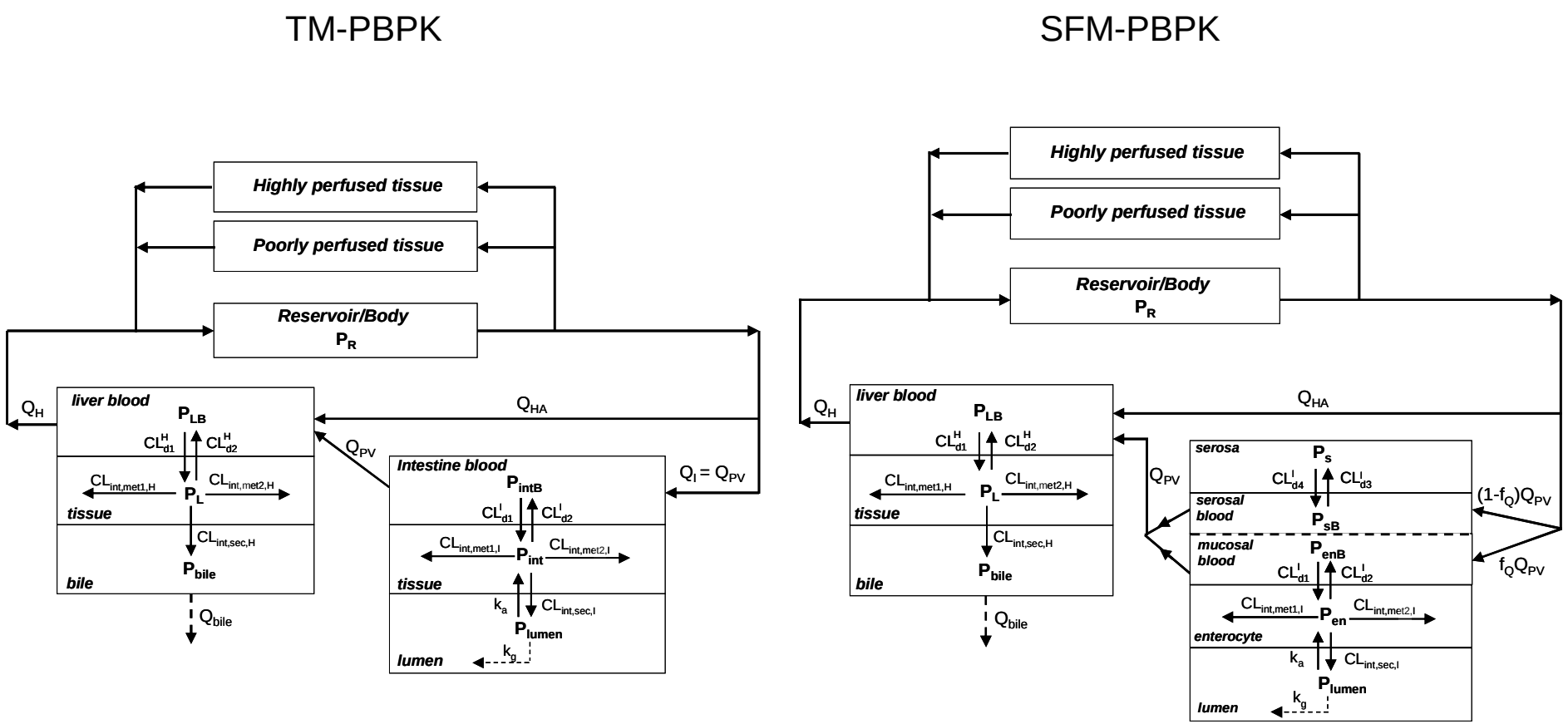

Figure 2

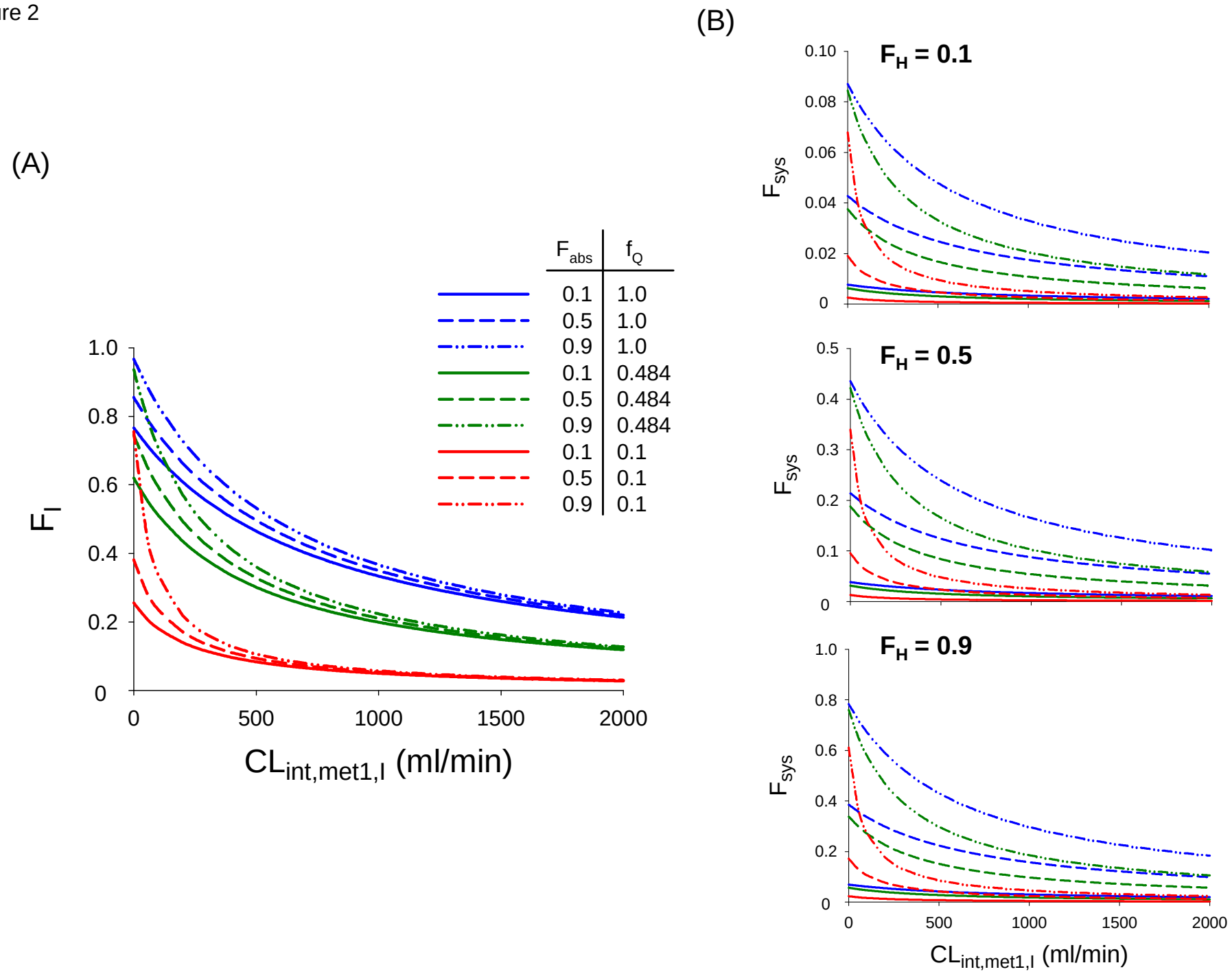

Figure 3

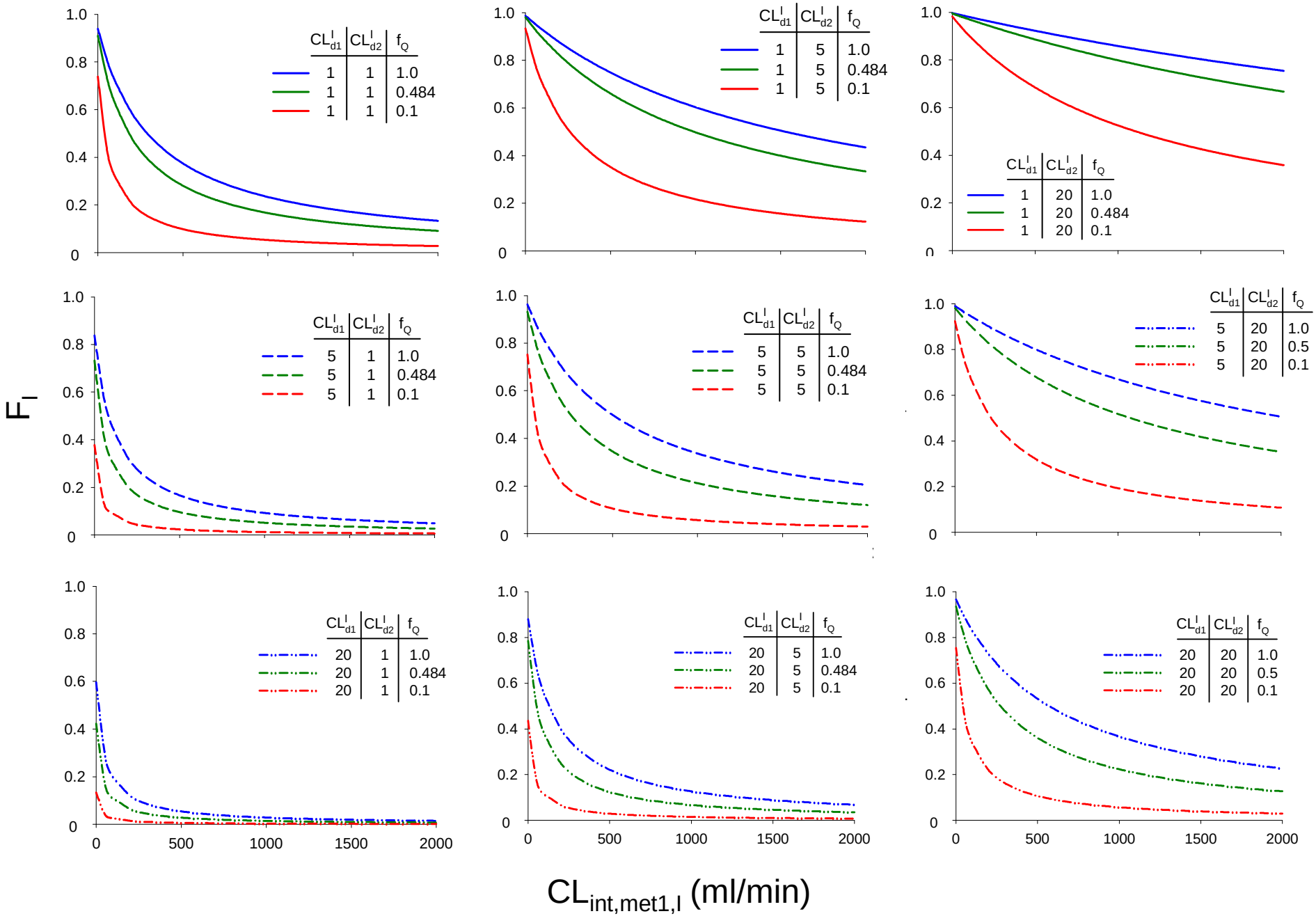

Figure 4

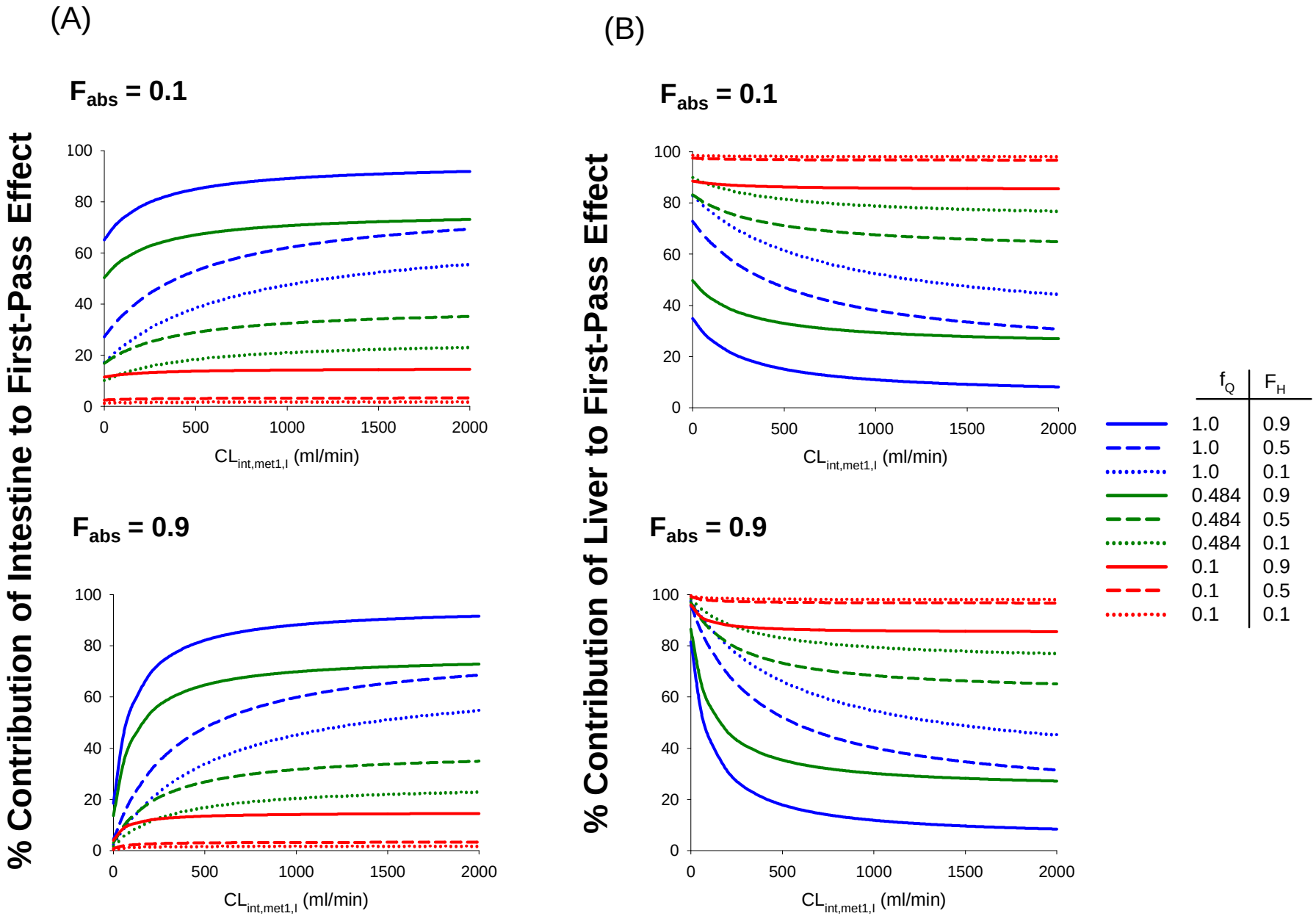

Figure 5